

# Crystallization of Calcium Phosphates. A Constant Composition Study

P. Koutsoukos, Z. Amjad, M. B. Tomson, and G. H. Nancollas\*

*Contribution from the State University of New York at Buffalo,  
Buffalo, New York 14214. Received June 21, 1979*

**Abstract:** The crystallization of the calcium phosphate phases from metastable supersaturated solutions upon seeding with highly crystalline and well-characterized seed material has been studied using a constant solution composition method. The activities of all ionic species in solution were maintained constant by the simultaneous addition of reagent solutions containing calcium, phosphate, and hydroxyl ions, controlled by a specific ion electrode. In solutions of low calcium phosphate concentration, supersaturated only with respect to the thermodynamically most stable hydroxylapatite (HAP), macroscopic amounts of this phase could be grown on HAP seed material without the formation of a precursor phase. These low rates of crystallization at a pH of 7.40 were measured with a precision hitherto unattainable. The influence of supersaturation, seed concentration, and the presence of fluoride ion has been investigated.

## Introduction

Although the precipitation of sparingly soluble salts is important in a wide variety of fields, the mechanism of the crystallization process is one of the least well understood phenomena in chemistry. In recent years there has been a resurgence of interest in the crystallization of inorganic salts from aqueous solution because of its involvement in areas such as the removal of phosphate from waste water, the fate of elements such as aluminum, calcium, iron, and other heavy metals in the formation of lake and ocean sediments, and in industry where the formation of scale on metal surfaces is a continuing problem. In desalination technology<sup>1,2</sup> the fouling of heat transfer surfaces by the growth of magnesium hydroxide and calcium salts such as the sulfate hydrates, carbonate polymorphs, and phosphates is a serious limitation to the use of evaporative techniques. Calcium phosphate formation is involved in many of these processes yet the stoichiometry of the precipitated phases is still poorly understood. It is now well established that the initially formed phase does not correspond to that of the final crystalline, thermodynamically stable hydroxylapatite,  $\text{Ca}_5(\text{PO}_4)_3\text{OH}$  (HAP).

Although the rates of homogeneous reactions in solution can often be predicted with considerable precision, for the heterogeneous precipitation process discrepancies amounting to orders of magnitude are not uncommon. In attempting to predict results of industrial precipitation processes, this frequently leads to overdesign of plants and expensive pilot plant studies. Crystallization in homogeneous solution can be considered to take place in two stages: nucleation and the growth of these nuclei to macroscopic dimensions. The initial stages of nucleation are difficult to investigate owing to problems associated with the detection of nuclei of atomic dimensions. Although there are numerous theories to describe the kinetics of precipitation,<sup>3-6</sup> the irreproducibility of most experimental studies of spontaneous precipitation makes it difficult to critically examine these theories. In this paper, we describe a method for the kinetic study of the precipitation of sparingly soluble salts from aqueous solution with an experimental reliability and theoretical relevance hitherto unobtainable.

In order to avoid many of the chance nucleation problems associated with attempts to attain homogeneous precipitation conditions, a highly reproducible seeded growth procedure was developed.<sup>7,8</sup> The method was used to study the kinetics of precipitation of a number of sparingly soluble salts such as silver chloride,<sup>7</sup> calcium sulfate hydrates,<sup>9</sup> calcium oxalate, an important renal stone constituent,<sup>10</sup> and barium sulfate, a scale component in many oil field situations.<sup>11,12</sup> Provided that special precautions are taken to avoid local concentration ef-

fects and the presence of foreign particles, it is possible to prepare supersaturated solutions which are stable for days. The addition of well-characterized seed crystals to the solutions enables their rate of growth to be studied by following concentration changes as a function of time. For many sparingly soluble salts  $\text{M}_{\nu+}\text{A}_{\nu-}$  the rate of crystallization can be expressed by an equation of the form

$$\frac{d[\text{M}_{\nu+}\text{A}_{\nu-}]}{dt} = -ks \left( \frac{[\text{M}^{m+}]^{\nu+} [\text{A}^{a-}]^{\nu-}}{[\text{M}^{m+}]_0^{\nu+} [\text{A}^{a-}]_0^{\nu-}} \right)^{1/\nu} \quad (1)$$

where  $[\text{M}^{m+}]$ ,  $[\text{A}^{a-}]$  and  $[\text{M}^{m+}]_0$ ,  $[\text{A}^{a-}]_0$  are the concentrations of crystal lattice ions in solution at time  $t$  and at equilibrium, respectively,  $k$  is the precipitation rate constant,  $s$  is proportional to the total number of available growth sites on the added seed material, and  $\nu = (\nu_+ + \nu_-)$ . The value of  $n$ , a constant, is typically 2 for the crystallization of a number of sparingly soluble salts.<sup>8-12</sup> The insensitivity of reaction rates to changes in fluid dynamics and the observed relatively high activation energy<sup>8-11</sup> point to a surface-controlled crystallization. Thus, although diffusion is usually regarded as the principal mechanism controlling the dissolution of crystals, it appears to play little part in the crystallization process.

Numerous studies have been made of the precipitation of calcium phosphates from solutions supersaturated with respect to four calcium phosphate phases in order of increasing solubility: HAP, tricalcium phosphate ( $\text{Ca}_3(\text{PO}_4)_2$ , TCP), octacalcium phosphate ( $\text{Ca}_8\text{H}_2(\text{PO}_4)_6 \cdot 5\text{H}_2\text{O}$ , OCP), and dicalcium phosphate dihydrate ( $\text{CaHPO}_4 \cdot 2\text{H}_2\text{O}$ , DCPD). The stoichiometric calcium/phosphate molar ratio of the initially precipitated phase does not correspond to the required value of 1.67 for the thermodynamically favored HAP. In order to reach the HAP composition extended solid-solution equilibrium is required and several theories have been put forward in an attempt to account for this phenomenon. DCPD was proposed as the precursor by Francis,<sup>13</sup> while the results of Posner and his co-workers<sup>14</sup> indicated an approximate composition of precursor corresponding to TCP. Brown<sup>15</sup> presented considerable X-ray and other evidence to show the existence of OCP in the physiological pH range and proposed this phase as a precursor to HAP formation.

In order to maintain the pH of the precipitating solution during calcium phosphate crystal growth, a pH-stat method was developed<sup>16</sup> in which base was added automatically during the course of the reaction. Similar pH and  $E_{\text{H}}$ -stated procedures have been described for studies of the precipitation and coagulation of aluminum hydroxide from pH 4 to 9.<sup>17</sup> The results of these and other studies again point to the formation

**Table I.** Constant Composition Calcium Phosphate Experiments (37 °C)

expt	$T_{Ca} \times 10^4$ , M	$T_{Ca}/T_p$	pH	HAP seed concn, mg L <sup>-1</sup>	titrant $T_{Ca} \times 10^3$ , M	$\Delta G$ DCPD, kJ mol <sup>-1</sup>	$\Delta G$ OCP, kJ mol <sup>-1</sup>	$\Delta G$ TCP, kJ mol <sup>-1</sup>	$\Delta G$ HAP, kJ mol <sup>-1</sup>	rate $\times 10^6$ , mol min <sup>-1</sup> m <sup>-2</sup> L
171	29.00	1.66	6.00	88.8	8.70	+0.6	+0.8	-0.6	-4.0	16.0
157	15.00	1.66	6.50	44.0	15.00	+0.5	+0.8	-0.6	-4.1	28.7
158	18.00	1.66	6.50	48.0	18.00	+0.4	+0.1	-1.7	-5.2	36.8
156	19.00	1.66	6.50	120.6	19.00	+0.8	+0.4	-1.3	-5.0	46.0
163	30.00	1.66	6.00	120.0	30.00	+0.3	+0.0	-1.8	-5.3	16.0
144	5.000	1.66	7.40	326.0	5.00	+1.9	+0.1	-2.2	-6.0	2.0
122	2.000	1.66	8.50	14.2	2.00	+3.4	+0.1	-3.2	-7.5	37.0
124	1.500	1.66	8.50	22.8	1.50	+4.0	+3.1	-2.5	-6.9	17.0
131	1.500	1.50	8.50	14.2	1.50	+3.9	+0.4	-2.6	-7.0	26.0
128	1.500	1.33	8.50	16.0	1.50	+3.7	+0.3	-2.7	-7.0	32.0
127	1.500	1.00	8.50	12.2	1.50	+3.4	+0.0	-3.0	-7.3	43.0
41	3.000	1.66	7.40	48.4 <sup>a</sup>	3.00	+2.9	+1.1	-1.1	-5.1	14.2
42	3.000	1.66	7.40	50.5 <sup>b</sup>	3.00	+2.9	+1.1	-1.1	-5.1	30.0
54	2.500	1.66	7.40	43.6 <sup>b</sup>	6.50	+3.3	+1.5	-0.6	-4.7	58.0
57	14.00	1.00	7.40	40.0	30.00	-0.4	-1.7	-4.2	-7.9	6764.2
61	12.00	1.33	7.40	16.7	26.67	+0.2	-1.2	-3.7	-7.4	382.1

<sup>a</sup> Human enamel seed material. <sup>b</sup> FAP seed material.

**Table II.** Experiment 138. Crystallization of HAP on HAP at 37 °C and pH 7.40<sup>a</sup>

sample no.	time, min	growth as % of original seed	$T_{Ca} \times 10^4$ , M	$T_p \times 10^4$ , M
29	0	0.0	9.000	5.400
30	180	35.0	8.986	5.400
31	240	81.0	8.985	5.400
32	300	129.0	8.968	5.400
33	360	174.0	9.000	5.420
10	420	221.0	9.032	5.416
11	480	268.0	8.969	5.402
12	520	300.0	8.995	5.408

<sup>a</sup> Titrants: (1) CaCl<sub>2</sub>, 1.170  $\times 10^{-2}$  M; (2) KH<sub>2</sub>PO<sub>4</sub>, 7.020  $\times 10^{-3}$  M; (3) KOH, 1.300  $\times 10^{-2}$  M. Seed concentration: 51.0 mg L<sup>-1</sup>.  $\Delta G(\text{HAP}) = -7.1$  kJ mol<sup>-1</sup>.  $\langle T_{Ca} \rangle = (8.991 \pm 0.022) \times 10^{-4}$  M.  $\langle T_p \rangle = (5.406 \pm 0.008) \times 10^{-4}$  M.

of metastable precursors in the overall precipitation reactions.

The difficulty of determining the stoichiometry of precipitation from the results of experiments such as those outlined above is due to the appreciable reduction in the concentrations of crystal lattice ions during the reactions. At each stage, the supersaturated solutions may therefore be metastable with respect to different phases which can form and subsequently redissolve as the concentrations decrease. In the precipitation of calcium phosphates, this probably accounts for the apparent variable stoichiometry and complex kinetics observed experimentally. Another problem is associated with the precision of the analytical determinations. The stoichiometric ratio,  $R$ , of a precipitated phase such as calcium phosphate is given by

$$R = \frac{T_{Ca_1} - T_{Ca_2}}{T_{p_1} - T_{p_2}} \quad (2)$$

where  $T_{Ca_1}$ ,  $T_{Ca_2}$ ,  $T_{p_1}$ , and  $T_{p_2}$  are the solution calcium and phosphate total concentrations at time  $t_1$  and  $t_2$ , respectively. From a propagation of error analysis of the typical uncertainties in the measured values, it can be shown that an analytical error of only a few percent can preclude differentiation between the different calcium phosphate phases which may act as precursors to the formation of HAP. Often, in order to improve the statistical reliability of the results, the initial supersaturation is increased in order to provide larger concentration differences. However, this can result in a change in the mechanism of the precipitation processes.<sup>18</sup>

These problems have been overcome in the method reported in the present paper, in which the precipitation is studied under

conditions of constant solution composition. The results provide direct evidence for OCP<sup>19</sup> as a precursor to HAP formation. Recent work has also shown that at pH 5.6 DCPD will grow preferentially from solutions supersaturated with respect to all calcium phosphate phases upon both natural and synthetic apatite.<sup>20</sup> At very low supersaturations, macroscopic quantities of stoichiometric, highly crystalline HAP can be formed.<sup>21</sup> The method enables the influence of pH, fluoride, seed type, and concentration to be studied with a precision hitherto unobtainable.

### Experimental Section

Reagent grade chemicals and triply distilled, CO<sub>2</sub>-free water were used and crystallization experiments were conducted in a nitrogen atmosphere. Phosphate standards were prepared from potassium dihydrogen phosphate (J. T. Baker Co., Ultrex) after drying at 105 °C and calcium chloride solutions were prepared from recrystallized analytical reagent grade calcium chloride (J. T. Baker Co.). Calcium and phosphate determinations were made by a combined method using an atomic absorption spectrometer (Perkin-Elmer Model 503) with a precision for calcium ( $\pm 0.2\%$ ) and for phosphate as vanadomolybdate ( $\pm 0.2\%$ ).<sup>22</sup> Specific surface areas (SSA) for seed as well as for the grown material were measured ( $\pm 1\%$ ) by a single point BET nitrogen adsorption using 30% nitrogen/helium mixture (Quantasorb II/Quantachrome, Greenvale, N.Y.). The HAP seed material, prepared as described previously,<sup>16</sup> had a molar  $T_{Ca}/T_p$  ratio of  $1.66 \pm 0.1$  and a SSA of  $36.1 \pm 0.1$  m<sup>2</sup> g<sup>-1</sup>. Unit cell lattice parameters ( $a = b = 9.418 \pm 0.002$  Å,  $c = 6.884 \pm 0.003$  Å) were determined by X-ray powder diffraction methods by using a Philips XRG3000 X-ray diffractometer. The seed was aged as a slurry for 4 months before use and was then filtered, dried, and stored as a powder. Fluorapatite (Ca<sub>5</sub>(PO<sub>4</sub>)<sub>3</sub>F, FAP) was prepared by adding sodium fluoride solutions to calcium hydroxide and phosphoric acid mixtures at a pH of 5.2. The seed material had a  $T_{Ca}/T_p$  molar ratio of  $1.67 \pm 0.1$  and a SSA of  $54 \pm 1$  m<sup>2</sup> g<sup>-1</sup>. Enamel seed material was prepared from human third molars by cleaning, separating the tooth components, grinding, and sieving (50–100 British Standard Mesh). The SSA was  $4.1 \pm 0.1$  m<sup>2</sup> g<sup>-1</sup> and the enamel powder was stored at 4 °C before use.

In a typical experiment, stable supersaturated solutions of calcium phosphate were prepared in a water-jacketed Pyrex cell and the pH was adjusted to the required value with dilute base. Nitrogen, saturated with water vapor, was bubbled through the solutions to exclude carbon dioxide. Following verification of the stability of the supersaturated solution, a known amount of well-characterized seed crystals was added to induce precipitation. The release of protons lowered the pH of the solution and a pH drop of approximately 0.003 triggered the addition of titrants from a pH-stat (Model 3D Metrohm, Brinkmann Instruments, Westbury, N.Y.). The pH was measured with a glass electrode–calomel electrode pair, standardized before and after each experiment with NBS standard buffer solutions prepared as follows: 0.025 *m* KH<sub>2</sub>PO<sub>4</sub> and 0.025 *m* Na<sub>2</sub>HPO<sub>4</sub>, pH 6.840, and

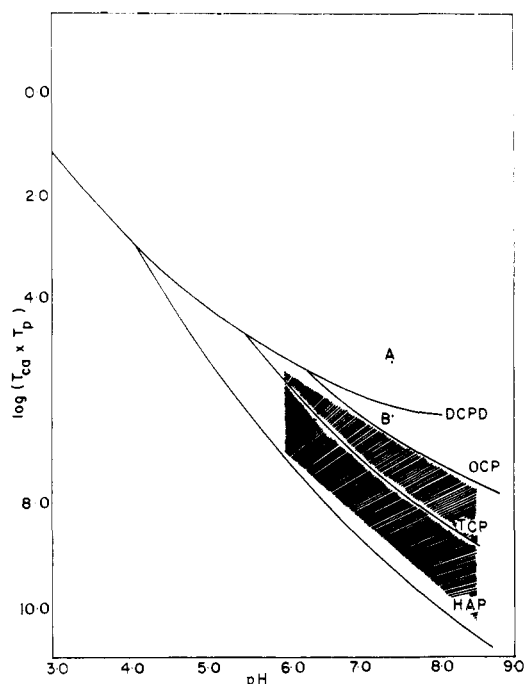


Figure 1. Logarithm of the product of calcium and phosphate concentrations plotted against pH values of solutions saturated with respect to various calcium phosphate phases in the ternary system  $\text{Ca}(\text{OH})_2\text{-H}_3\text{PO}_4\text{-H}_2\text{O}$ . Calculated for 37 °C.

0.008 695 *m*  $\text{KH}_2\text{PO}_4$  and 0.030 43 *m*  $\text{Na}_2\text{HPO}_4$ , pH 7.384 at 37 °C. The addition of titrant was monitored and, in addition, samples were withdrawn from the supersaturated solutions, filtered (0.22- $\mu\text{m}$  filter, Millipore, Bedford, Mass.), and analyzed for calcium and phosphate. The solid phases, withdrawn from time to time, were air- or freeze-dried and examined by scanning electron microscopy (ISI, Model Super II, tilt angle of 40°), SSA, infrared (Perkin-Elmer 467 spectrophotometer), and X-ray analysis.

In the conventional pH-stat experiments, with a dilute standard potassium hydroxide solution as titrant, the lattice ion concentrations were allowed to decrease with time. In the method reported here, however, the glass electrode in the solutions was used to trigger the simultaneous addition of reagent solutions from mechanically coupled motor-driven automatic burets. The addition of reagents compensated for the change in anion and cation concentrations and the required concentrations of titrant solutions were determined from the results of preliminary experiments. By adding inert electrolyte (potassium chloride) to the supersaturated solution and to the titrants, the ionic strength was also maintained constant to within 1%. This was necessary since changes in activity coefficients could also trigger the addition of reagent solutions. Using the technique outlined here, it was possible to study the rates of crystallization, as given by the rates of addition of reagent solutions with a precision of approximately 3%. At constant solution compositions, the stoichiometry of the precipitated phase is given by the molar ratios of the titrant solutions; this was 1.66 for all experiments with the exception of experiments 57 and 61.

## Results and Discussion

The concentrations of ionic species in the supersaturated solutions at any time were calculated from mass balance, electroneutrality, proton dissociation, and calcium phosphate ion-pair association constants by successive approximations for the ionic strength, *I*. The activity coefficients of *z*-valent species were calculated from the extended form of the Debye-Hückel equation proposed by Davies.<sup>23</sup> Values used for the dissociation constants of phosphoric acid at 37 °C were  $k_1 = 5.861 \times 10^{-3} \text{ mol L}^{-1}$ ,  $k_2 = 6.839 \times 10^{-8} \text{ mol L}^{-1}$ , and  $k_3 = 6.607 \times 10^{-13} \text{ mol L}^{-1}$ <sup>24</sup> and for the calcium phosphate complexes  $K^\circ(\text{CaHPO}_4) = 6.81 \times 10^2 \text{ L mol}^{-1}$ ,  $K^+(\text{CaH}_2\text{PO}_4^+) = 31.9 \text{ L mol}^{-1}$ ,<sup>25</sup> and  $K(\text{CaOH}^+) = 25.4 \text{ L mol}^{-1}$ .<sup>26</sup> The solubility product values at 37 °C were

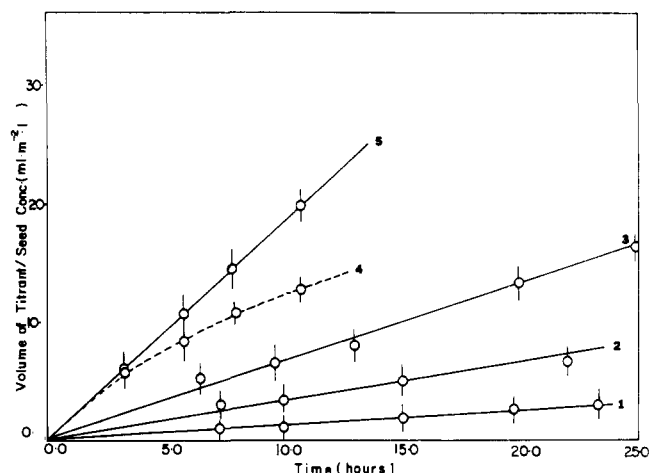


Figure 2. Growth of HAP crystals. Plots of titrant added as a function of time for different supersaturations, corrected for seed material changes with the exception of curve 4. Curve 1,  $T_{\text{Ca}} = 2.90 \times 10^{-3} \text{ M}$ ,  $T_{\text{p}} = 1.74 \times 10^{-3} \text{ M}$ , pH 6.0; curve 2,  $T_{\text{Ca}} = 1.50 \times 10^{-3} \text{ M}$ ,  $T_{\text{p}} = 0.90 \times 10^{-3} \text{ M}$ , pH 6.50; curve 3,  $T_{\text{Ca}} = 1.80 \times 10^{-3} \text{ M}$ ,  $T_{\text{p}} = 1.08 \times 10^{-3} \text{ M}$ , pH 6.50; curves 4 and 5, expt 156 (Table I).

$K_{\text{so}}(\text{DCPD}) = 1.87 \times 10^{-7}$ ,<sup>27</sup>  $K_{\text{so}}(\text{OCP}) = 8.3 \times 10^{-48}$  (from ref 28, corrected for ion-pair formation),  $K_{\text{so}}(\text{TCP}) = 2.83 \times 10^{-30}$ ,<sup>29</sup> and  $K_{\text{so}}(\text{HAP}) = 2.35 \times 10^{-59}$ .<sup>30</sup>

In Figure 1, the calculated products  $\log(T_{\text{Ca}}T_{\text{p}})$  for equilibrium with respect to each of the calcium phosphate phases are plotted as a function of pH.

The results of some typical experiments are summarized in Table I, in which the driving force for crystallization (eq 2) is expressed as a Gibbs free energy of transfer from supersaturated to saturated solution for each of the calcium phosphate phases.

$$\Delta G = \frac{-RT}{\nu} \ln \text{IP}/K_{\text{so}} \quad (3)$$

In eq 3, IP is the activity product in the supersaturated solution,  $K_{\text{so}}$  is the value of IP at equilibrium, and  $\nu$  is the number of ions in the molecule. All experiments with the exception of 57 and 61 lie in the shaded region of Figure 1. In experiment 61, 1 mL of a slurry (8 mg seed  $\text{L}^{-1}$ ) was used to initiate crystallization; in the other experiments dry seed was used. Results of a typical calcium phosphate experiment (138 in Table II) show that the amount of solid phase was more than tripled with no significant variation of  $T_{\text{Ca}}$  and  $T_{\text{p}}$  in the growth solution. Typical plots of mixed titrant added as a function of time are shown in Figure 2. Correction of raw data (e.g., experiment 156, dotted line) for solid concentration changes during the experiments yielded the excellent linear plots shown over a range of solution supersaturations. From Table I and Figure 3 it can be seen that the rate of crystallization is proportional to the concentration of inoculating seed, thus confirming that crystallization occurred only on the added seed material without any secondary nucleation or spontaneous precipitation. The results of experiments 124, 131, 128, and 127 in Table I indicate that the stoichiometry of the precipitated phase is not dependent upon the  $T_{\text{Ca}}/T_{\text{p}}$  ratio in the supersaturated solution. In these experiments both TCP and HAP are thermodynamically favored but the formation of TCP has never been convincingly demonstrated under these experimental conditions.

The decrease in SSA during the precipitation reactions, shown in Figure 4 (from 36.1 to 20.0  $\text{m}^2 \text{g}^{-1}$ ), reflects the improved crystallinity of the solid phase. This was confirmed by scanning electron microscopy and X-ray diffraction.

The influence of FAP as seed material in supersaturated solutions of calcium phosphate in the presence and in the absence of fluoride ion is illustrated by the results of experiments

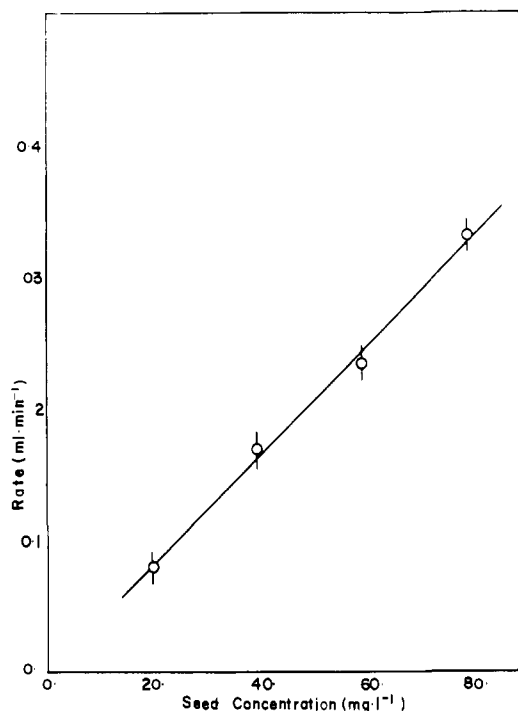


Figure 3. Crystal growth of hydroxylapatite. Plot of rate of growth as a function of seed concentration.

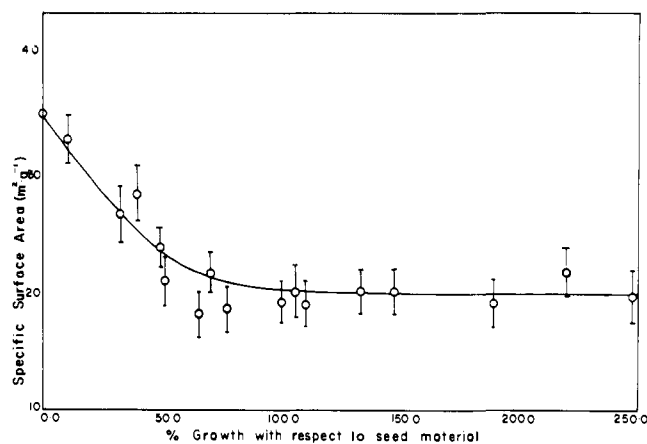


Figure 4. Plot of specific surface area as a function of extent of growth with respect to original seed.

42 and 54 in Table I. In experiment 42, pure HAP was formed on the surface of the FAP seed, whereas, in the presence of 5 ppm of fluoride (experiment 54), FAP was formed exclusively. It can be seen in Figure 5 that the human enamel seed will also induce the growth of HAP but at a rate lower than that for FAP or HAP. Table III shows the results of a typical experiment in which a fluoride ion electrode was used to control the rate of addition of calcium phosphate and fluoride titrants during the crystallization of FAP on FAP seed in the presence of fluoride ion. It is interesting to note that this electrode maintains the composition of the supersaturated solution to within close limits despite the fact that it does not have a sufficiently rapid response to faithfully reflect concentration changes during more conventional precipitation reactions.

Crystallization results at higher concentrations in calcium phosphate solutions supersaturated with respect to other phases are illustrated by experiments 57 and 61 in Table I, represented by points A and B, respectively, in Figure 1. In experiment 61 a preliminary study using titrant molar ratios,  $T_{Ca}/T_p$ , of 1.45 resulted in a 6% decrease in  $T_{Ca}$  in the first 40 min of re-

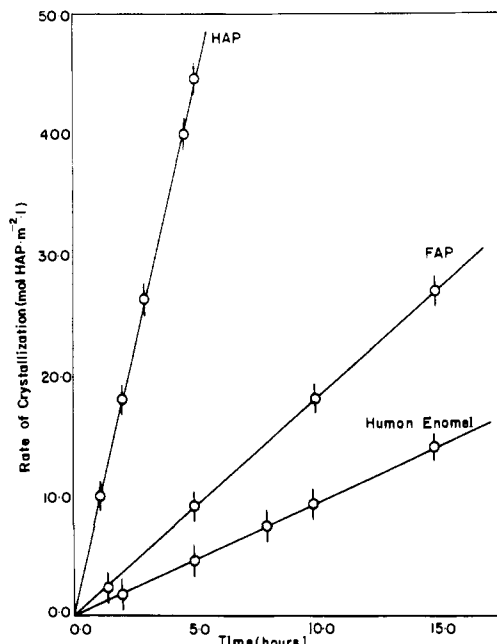


Figure 5. Plot of rate of crystallization as a function of time for different seed materials.

action. A change of the  $T_{Ca}/T_p$  ratio of the titrant solutions from 1.45 to 1.33 resulted in crystallization with  $T_{Ca}$  and  $T_p$  in the supersaturated solution constant to within  $\pm 0.1\%$  for 10 min of growth. During this period, more than five times the added initial seed material had precipitated and X-ray and IR studies confirmed the formation of OCP. At a lower pH of 6.00 (see Figure 1) DCPD was used as seed material and with a  $T_{Ca}/T_p$  of 1.00 the calcium and phosphate concentrations were maintained constant for several hours of growth while some 15 times the original seed material was precipitated on the added crystals. SEM and X-ray data indicated the exclusive formation of DCPD on the seed crystals which increased in size during the first 2 h of growth. Following this time period, scanning electron microscopy showed a roughening of the crystal surface indicating surface nucleation of additional DCPD. Secondary nucleation is important in many industrial processes. The constant solution composition method, described here, enables studies to be made under highly reproducible conditions.

The results presented in Table II show that it is possible to prepare measurable quantities of stoichiometric HAP in the laboratory at typical physiological calcium phosphate concentrations. Extended experiments (e.g., experiment 138 over a period of 9 h) have resulted in the growth of solid amounting to more than three times the initial seed used to inoculate the supersaturated solutions. Macroscopic amounts of highly crystalline HAP and FAP, over a wide range of pH from 6.0 to 8.5 (shaded area, Figure 1), have been prepared without the involvement of precursor phases. Since the concentrations remain constant during the experiments, the analytical techniques used for verification can be optimized with greatly improved precision. In addition, the method may be used with specific ion electrodes other than hydrogen and fluoride. Thus the calcium electrode, which does not respond sufficiently rapidly for use in situations in which the calcium concentration falls rapidly with time, has been used to study calcium oxalate precipitations at constant composition.<sup>31</sup> The ability to hold the supersaturation at a constant value for long periods of time in order to determine the stoichiometry of the precipitated phase will be particularly useful in other phosphate systems such as iron and aluminum.

The rates of crystallization of HAP in solutions of low supersaturation at pH values of 7.4 and 8.50 are plotted ac-

**Table III.** Constant Composition, FAP Growth Using Fluoride Electrode<sup>a,b</sup>

sample no.	time, min	emf, F <sup>-</sup> electrode, mV	titrant vol, mL	FAP grown as % of original seed	T <sub>Ca</sub> × 10 <sup>4</sup> , M	T <sub>p</sub> × 10 <sup>4</sup> , M
1	0	35.4	0.0	0.	2.50	1.50
2	0	35.4	0.0	0.	2.50	1.50
3	45	35.4	10.2	31.	2.54	1.56
4	75	35.4	20.2	61.	2.52	1.51
5	107	35.8	30.3	91.	2.50	1.50
6	137	35.6	50.5	152.	2.52	1.51
7	170	35.8	63.3	190.	2.52	1.52

<sup>a</sup> Titrants: (1) CaCl<sub>2</sub> = 6.50 × 10<sup>-3</sup> M; (2) KH<sub>2</sub>PO<sub>4</sub> = 3.90 × 10<sup>-3</sup> M + 1.68 × 10<sup>-3</sup> M NaF + 7.47 × 10<sup>-3</sup> M KOH. Seed: 20.4 mg HAP/500 mL. (T<sub>Ca</sub>) = (2.52 ± 0.01) × 10<sup>-4</sup> M. (T<sub>p</sub>) = (1.52 ± 0.02) × 10<sup>-4</sup> M. <sup>b</sup> 5 ppm of F<sup>-</sup> in solution.

**Table IV.** Unit Cell Parameters of HAP Grown Phases<sup>c</sup>

expt	duration, h	T <sub>Ca</sub> × 10 <sup>4</sup> , M	T <sub>Ca</sub> /T <sub>p</sub>	[KCl] × 10 <sup>3</sup> , M	a = b, Å	c, Å	growth, % initial seed
70	20	3.00	1.66	2.00	9.423 ± 0.007	6.726 ± 0.003	600
91	7	3.00	1.66	2.00	9.443 ± 0.002	6.887 ± 0.002	200
130	26	1.50 <sup>a</sup>	1.33 <sup>b</sup>	0.00	9.413 ± 0.002	6.884 ± 0.005	80
129	20	4.00	1.66	2.67	9.400 ± 0.011	6.880 ± 0.008	60
110	169	5.00	1.66	3.30	9.383 ± 0.008	6.792 ± 0.01	250

<sup>a</sup> T<sub>Ca</sub> as Ca(OH)<sub>2</sub>. <sup>b</sup> T<sub>p</sub> as H<sub>3</sub>PO<sub>4</sub>. <sup>c</sup> HAP seed material used for the experiments.

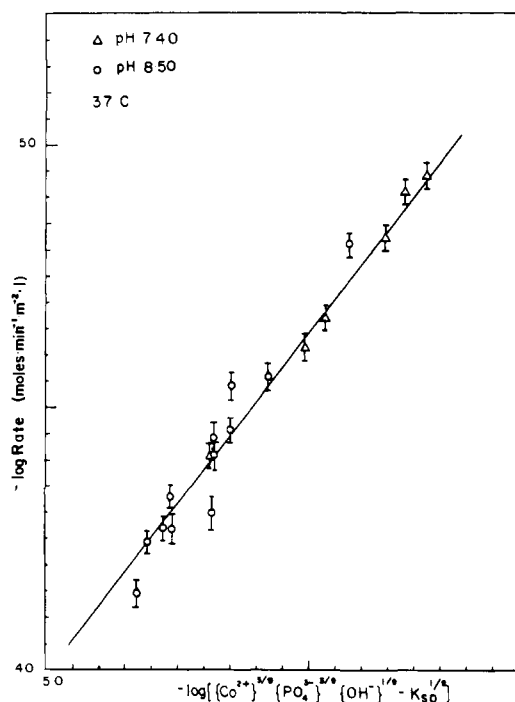


**Figure 6.** Crystal growth of hydroxylapatite. Plot of log (rate) against log [(Ca<sup>2+</sup>)<sup>5/9</sup>(PO<sub>4</sub><sup>3-</sup>)<sup>3/9</sup>(OH<sup>-</sup>)<sup>1/9</sup> - K<sub>sp</sub><sup>1/9</sup>] where braces indicate activities of the species enclosed.

cording to the kinetic equation (1) in Figure 6. The slope of the line corresponds to an effective order of reaction,  $n = 1.25 \pm 0.02$ . It is interesting to note that, when the crystallization of HAP was allowed to proceed for extended times (Table IV, experiments 70 and 110), the  $c$  axis of the grown phase decreased below the value, 6.88 Å, for pure HAP. It has been suggested that this reflects the presence of chloride in the apatite lattice.<sup>32,33</sup> Experiments (129 and 130 in Table IV) in the

absence of chloride ion, using calcium hydroxide and phosphoric acid for titrant and supersaturated solution preparation, yielded solid HAP phases with normal  $c$ -axis values.

**Acknowledgments.** We thank the National Institute of Dental Research for a grant (DE 03223) in support of this work.

#### References and Notes

- (1) Spiegler, K. S. S. "Salt-Water Purification"; Wiley: New York, 1962; Chapter 4.
- (2) Elliot, M. N. *Desalination* **1969**, *6*, 87; **1970**, *8*, 22.
- (3) Hahuest, M.; Kleber, W. *Kolloid Z.* **1959**, *11*, 1512.
- (4) Stranski, I. N. *Z. Phys. Chem., Abt. A* **1928**, *136*, 259.
- (5) Becker, R.; Doring, W. *Ann. Phys. (N.Y.)* **1935**, *24*, 719.
- (6) Becker, R. *Discuss. Faraday Soc.* **1949**, *5*, 50.
- (7) Davies, C. W.; Jones, A. L. *Discuss. Faraday Soc.* **1949**, *5*, 103.
- (8) Nancollas, G. H.; Purdie, N. *Q. Rev., Chem. Soc.* **1964**, *18*, 1.
- (9) Nancollas, G. H.; Reddy, M. M.; Tsai, F. *J. Cryst. Growth* **1973**, *20*, 125.
- (10) Gardner, G. L.; Nancollas, G. H. *J. Cryst. Growth* **1974**, *21*, 267.
- (11) Liu, S. T.; Nancollas, G. H. *J. Cryst. Growth* **1970**, *6*, 281.
- (12) Liu, S. T.; Nancollas, G. H. *Pet. Eng. J.* **1975**, 509.
- (13) Francis, M. D. *Ann. N.Y. Acad. Sci.* **1965**, *131*, 694.
- (14) Eanes, E. D.; Gillissen, I. H.; Posner, A. S. *Proc. Int. Conf. Cryst. Growth* **1966**, 373.
- (15) Brown, W. E. *Clin. Orthop. Relat. Res.* **1966**, *44*, 205.
- (16) Nancollas, G. H.; Mohan, M. S. *Arch. Oral Biol.* **1970**, *15*, 731.
- (17) Stumm, W.; Morgan, J. J. *J. Am. Water Works Assoc.* **1962**, *54*, 971.
- (18) Nancollas, G. H.; Tomazic, B. *J. Phys. Chem.* **1974**, *78*, 2218.
- (19) Tomson, M. B.; Nancollas, G. H. *Science* **1978**, *200*, 1059.
- (20) Barone, J. P.; Nancollas, G. H. *J. Colloid Interface Sci.* **1977**, *62*, 421.
- (21) Amjad, Z.; Koutsoukos, P.; Tomson, M. B.; Nancollas, G. H. *J. Dent. Res.* **1978**, *57*, 909.
- (22) Tomson, M. B.; Barone, J. P.; Nancollas, G. H. *At. Absorpt. Newsl.* **1977**, *16*, 117.
- (23) Davies, C. W. "Ion Association"; Butterworths: London, 1962.
- (24) Bates, R. G. *J. Res. Natl. Bur. Stand.* **1951**, *47*, 127.
- (25) Marshall, R. W.; Nancollas, G. H. *J. Phys. Chem.* **1969**, *73*, 3838.
- (26) Gimblett, F. G.; Monk, C. B. *Trans. Faraday Soc.* **1954**, *50*, 965.
- (27) Marshall, R. W. Ph.D. Thesis, State University of New York at Buffalo, 1970.
- (28) Moreno, E. C.; Brown, W. E.; Osborn, G. *Soil Sci. Proc.* **1960**, 99.
- (29) Gregory, T. M.; Moreno, E. C.; Patel, J.; Brown, W. E. *J. Res. Natl. Bur. Stand., Sect. A* **1974**, *78*, 667.
- (30) McDowell, H.; Gregory, T. M.; Brown, W. E. *J. Res. Natl. Bur. Stand., Sect. A* **1977**, *81*, 273.
- (31) Sheehan, M.; Nancollas, G. H. *Invest. Urol.*, in press.
- (32) McConnell, D. C. "Apatite"; Springer-Verlag: New York, 1973; p 47.
- (33) Legeros, R. Z. *Arch. Oral Biol.* **1974**, *20*, 63.